Available online at www.sciencedirect.com
ScienceDirect
International Journal of Thermal Sciences 47 (2008) 1482–1489
International Journal of Thermal Sciences
www.elsevier.com/locate/ijts

Steady and transient thermo-hydraulic performance of disc with tree-shaped micro-channel networks with and without radial inclination

B.V.K. Reddy, P.V. Ramana, Arunn Narasimhan *

Heat Transfer and Thermal Power Laboratory, Department of Mechanical Engineering, Indian Institute of Technology Madras, Chennai 600036, India

Received 21 August 2007; received in revised form 14 November 2007; accepted 15 November 2007

Available online 15 January 2008

Abstract

Steady and transient conjugate heat transfer and fluid flow through tree-shaped radially branching micro-channel networks, embedded in a disk-shaped heat sink, are investigated using numerical simulations. The typical dimensions of the disk are taken as 20 mm radius and 2 mm thickness while the hydraulic diameters of the micro-channel network are in the range of 0.67–0.44 mm, with a constant 0.5 mm height. In steady state, increased levels of complexity of the tree network result in more uniform temperature distribution in the disc ($\bar{T}_{\max} \to \bar{T}_{\text{avg}}$). However the degree of reduction in temperature reduces for higher complexity. Using the steady state result for minimal flow resistance that yields minimal thermal resistance for heat transfer, the transient response of the disk with differing levels of tree complexities is shown to behave more uniformly under similar imposed heat transfer load. The effect of radial inclination of the flow tree channels on the overall pressure drop of the coolant flow and the disk temperature distribution is also investigated. By allowing 0.1 mm radial inclination to the channel network shows 45 percent reduction in pressure drop for the first level of branching complexity ($k = 1$, $n = 3$) and 25 percent for the highest level ($k = 4$, $n = 3$) as compared to the corresponding planar channel.

Keywords: Micro-channel; Constructal; Tree-shaped network; Pump power; Transient; Forced convection; Electronics cooling; Disk heat sink

1. Introduction

It is established that the temperature of electronic devices has a strong impact on their reliability and performance [1] and they need to be maintained below 80–110 °C. Cooling options using disks embedded with conventional straight and parallel rectangular cross-section micro-channel networks posses two inherent drawbacks, namely high-pressure drop requirement and uneven temperature distribution. Following the evolution of natural systems, it is shown in Bejan [2,3], and Bejan and Errera [4] that when competing global and local constraints operate, the optimal geometric design often is engineered to become a tree structure. Applying this idea, treating the minimization of temperature difference (thermal resistance) along with the flow resistance, Wechsatol et al. [5] showed that in a uniformly heat generating disc cooled by a flow, the optimal flow path evolves into a tree shaped network as the flow reaches steady state. Further analysis for radial tree-shaped flow channels on disks have been reported in Wechsatol et al. [6], while Rocha et al. [7] discussed about the application of tree-shaped networks for electronics cooling proposing geometries for minimal flow resistance.

Micro-channel heat sinks are emerging as one of the optimal solutions for electronics cooling applications in the present scenario. Tuckerman and Pease [8] built a water-cooled heat sink with micro channels capable of receiving up to a heat flux of 790 W cm^{-2}. Chen and Cheng [9] showed the fractal nature of tree-shaped micro-channel networks used in cooling electronics. Senn and Poulikakos [10] investigated laminar mixing effects on the thermo-hydraulics of tree-shaped micro-channel networks and their cooling applications in fuel cells.

In this study the concept of tree-shaped networks is utilized to optimize the flow and thermal resistance of micro-channels embedded in a disk for cooling electronics. This has been explored by Wang et al. [11] in a recent study for a specific disk geometry and flow rate of the coolant under steady state. In

* Corresponding author. Tel.: +91 44 22574696.
E-mail address: arunn@iitm.ac.in (A. Narasimhan).

1290-0729/$ – see front matter
doi:10.1016/j.ijthermalsci.2007.11.003

Nomenclature

A	surface area	m^2	
b	number of bifurcations at the end of each channel		
c_p	specific heat	$J\,kg^{-1}\,K^{-1}$	
D_h	hydraulic diameter	m	
d	thickness of the disk	m	
$\bar{h}$	height of the channel (h/R), nondimensional		
H	height of the channel	m	
l	length variation along the dashed line, Fig. 2		
L	length of the channel	m	
$\bar{L}$	length of the channel (l/L_k), nondimensional		
k	lower order branching level at the bifurcation		
M	mass flow rate ($\dot{m}c_p/(\lambda_s d)$), nondimensional		
$\dot{m}$	mass flow rate	$kg\,s^{-1}$	
n	number of bifurcations at the center of the disk		
p	pressure	$N\,m^{-2}$	
$\bar{P}$	pressure ($(P_{in}-P_{out})/(\frac{1}{2}\rho v_{in}^2)$), nondimensional		
q	heat current ($q''\pi R^2$)	W	
q''	heat flux	$W\,m^{-2}$	
q^*	heat flux ($q''/(q_0''=250\,kW\,m^{-2})$), nondimensional		
R	radius of disc	m	
$\bar{r}$	radius (r/R), nondimensional		
Re	Reynolds number (vD_h/ν)		
t	time	s	
T	temperature	K	
$\bar{T}$	temperature ($(T-T_{in})/(q/\lambda_s d)$), nondimensional		
v	velocity	$m\,s^{-1}$	
V	volume of the disk	m^3	
W	width of the channel	m	
x, y, z	coordinates	m	
X	projected length of channel on x coordinate	m	

Greek symbols

θ	angle	degrees
λ	thermal conductivity	$W\,m^{-1}\,K^{-1}$
μ	dynamic viscosity	$N\,s\,m^{-2}$
ρ	density	$kg\,m^{-3}$
τ	time ($\alpha_s t/R^2$), nondimensional	
ξ, η	tangential and normal coordinates to the surface, Fig. 2	

Subscripts

avg	average
b	bulk fluid
btm	bottom
ch	channel
cr	critical
f	fluid
in	inlet
incl	inclination
max	maximum
out	outlet
s	solid

general, owing to the nature of the electronics being cooling, these disks with tree networks would be subjected to transient thermal condition during the periodic start-up or shut-down of the device. Irrespective of their geometric branching complexity, knowledge of the transient performance of such cooling tree networks becomes essential to operate the electronics at or below their Set Point Temperature (SPT = 90 °C) limit. The present study generates the critical minimal mass flow rate required in steady state for the safe operation of the disk (i.e. $T_{max} < T_{SPT}$) for several imposed heat fluxes, under increasing levels of complexity. These minimal mass flow rates (minimal flow resistance) are used to study the transient system performance. Further, as an option for minimizing further the overall pressure-drop, the flow channel inclination effect is also investigated.

2. Geometry and governing equations

The configuration shown in Fig. 1 is the considered tree-shaped radial branching micro-channel network grooved on silicon disk of 20 mm in radius and 2 mm thickness for all the levels ($k = 1$ to 4). Fig. 2 depicts the two dimensional view of level $k = 4$ of disk in Fig. 1. The dimensions of the micro-channels are optimized based upon the two constraints of fixed total volume and fixed channel volume in order to minimize the global flow resistance of the path as shown in Bejan [3]. The

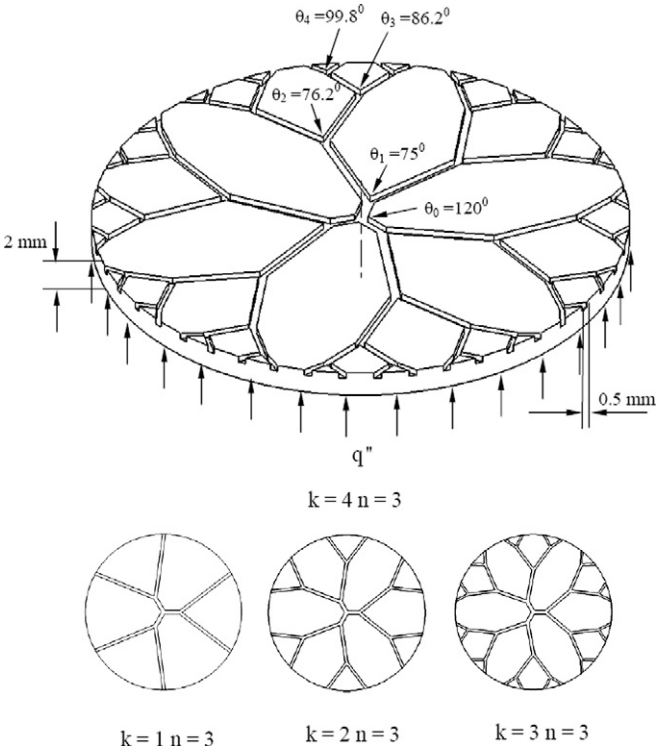

Fig. 1. Schematic diagram of three-dimensional geometry of disk with grooved tree structured micro-channels for levels $k = 1$ to 4, $n = 3$.

Table 1
Typical micro-channel dimensions in mm, as calculated from Wechsatol et al. [16]

	k	H	W	D_h	X	θ (°)	L
$k=0$	0	0.5	1	0.6667	20	120	20
$k=1$	0	0.5	1	0.6667	4.28	120	4.28
	1	0.5	0.7937	0.6135	15.72	74.94	16.44
$k=2$	0	0.5	1	0.6667	3.14	120	3.14
	1	0.5	0.7937	0.6135	9.64	38.85	10.18
	2	0.5	0.6300	0.5575	7.22	36.77	8.64
$k=3$	0	0.5	1	0.6667	3.06	120	3.06
	1	0.5	0.7937	0.6135	7.76	40.6	8.32
	2	0.5	0.6300	0.5575	6.22	36.79	7.36
	3	0.5	0.5	0.5	2.96	42.39	3.88
$k=4$	0	0.5	1	0.6667	2.18	120	2.18
	1	0.5	0.7937	0.6135	8.04	37.5	8.4
	2	0.5	0.6300	0.5575	5.84	38.1	6.74
	3	0.5	0.5	0.5	2.78	43.1	3.6
	4	0.5	0.3968	0.4425	1.16	49.8	1.736

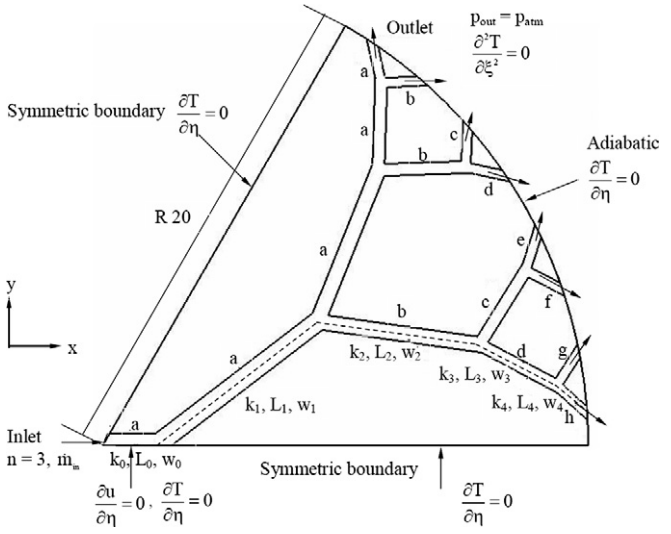

Fig. 2. Two-dimensional computational domain is 1/6th comprising part of the full geometry of level $k=4$, $n=3$, shown in Fig. 1.

optimized dimensions of the different levels of the tree structure networks are given in Table 1. As suggested in Wechsatol et al. [5], based on the Murray's law [12], in the laminar flow case, the hydraulic diameters of branching ratios can be written as

$$\frac{D_{k+1}}{D_k} = b^{-1/3} \tag{1}$$

where, b is the number of branches into each channel split, for the present analysis, $b=2$ and k represents the lower order branching level at the bifurcation (see Fig. 1). The procedure suggested in Pence and Enfield [13] can be extended further to rectangular cross section channel to find the widths or lengths of branching ratios for fixed height, as

$$\frac{W_{k+1}}{W_k} = b^{-1/3} \tag{2}$$

$$\frac{L_{k+1}}{L_k} = b^{-1/3} \tag{3}$$

As shown in Fig. 1, the cooling flow network branches out from the center of the disk into three channels ($n=3$) and each channel bifurcates into two ($b=2$) at each level (k). The values of $k=0$ to 4, with $k=0$ representing the straight radial channel, determine the increasing complexity of the network from the center to the periphery of the disk. Observe in Fig. 2 the sub-channels at each branch are denoted using letters a to h. For example, at $k=2$, the corresponding sub-channels are labeled as a, b and c so that $k=2a$, $k=2b$ and $k=2c$ represent respectively, the individual section of the channel. As shown in Fig. 1 the bottom wall of the disk is subjected to constant heat flux q''. The disk is cooled in time by a steady, laminar fluid flow in the channels, with fixed inlet mass flow rate ($\dot{m}$, kg s^{-1}) and temperature T_{in}. Use of the Navier–Stokes equations in predicting the flow and heat transfer behavior in micro-channels has been validated by many recent studies including Liu and Garimella [14], Judy et al. [15] and Qu and Mudawar [16] with good agreement found between the measurements and numerical predictions. Hence the governing equations for mass, momentum and energy are solved using numerical methods in the present study for both solid and fluid domain of the disk shown in Fig. 1 and are as follows.

- Continuity equation:

$$\nabla.\vec{v} = 0 \tag{4}$$

- Momentum equation:

$$\rho(T)\frac{D\vec{v}}{Dt} = \nabla p + \nabla.\left(\mu(T)\nabla\vec{v}\right) \tag{5}$$

- Energy equation:
  - Fluid region:

$$\rho(T)c_p(T)\frac{DT}{Dt} = \nabla.\left(\lambda(T)\nabla T\right) \tag{6}$$

  - Solid region:

$$(\rho c)_s\frac{\partial T_s}{\partial t} = \nabla.(\lambda_s\nabla T_s) \tag{7}$$

The above governing equations are solved in the solid and liquid regions of the disk with the boundary conditions in Fig. 2

along with constant heat flux ($q'' = \text{constant}$) imposed at the bottom of the heat sink, constant mass flow at the inlet of the channel ($\dot{m} = \text{constant}$), pressure outlet (gauge pressure, $p = 0$) imposed at the periphery (outlet) of the disk and adiabatic conditions imposed at the remaining exposed surfaces of the disk.

3. Solution methodology

Numerical simulation are performed using a finite volume formulation of Eqs. (4) to (7) with a second order upwind scheme of iterative solution with the pressure and velocity terms of Eqs. (4) and (5) coupled using the SIMPLE algorithm [17]. Suitable grid and time step size were chosen after performing grid and time step independence tests of the numerical results for all the tree complexity levels ($k = 0$ to 4). Owing to journal printing space constraints, only sample grid and time step independence results for the level $k = 2$ and $n = 3$ (see Fig. 1) are reported in Tables 3 and 4 respectively. Based on these results, for level $k = 2$, the grid size with 311 158 cells and the time step 0.025 were used to generate further results. The numerical simulation takes into account the temperature dependent property variation in the fluid (water, Table 2) while constant properties are considered for the silicon substrate (Table 2).

Table 2
Properties of liquid water (in SI units) at atmospheric pressure ($273.15 < T < 373.15$ K) [1] and properties of silicon (in SI units) at 310 K used in the simulation

$\rho(T)$	$999.8396 + 18.22494T - 7.92221 \times 10^{-3}T^2 - 5.54485 \times 10^{-5}T^3 + 1.4956 \times 10^{-7}T^4 - 3.93295 \times 10^{-10}T^5/(1 + 1.8159 \times 10^{-2}T)$ where T in °C
$\mu(T)$	$2.414 \times 10^{-5} \times 10^{247.8/(T-140)}$ where T in K
$c_p(T)$	$8958.9 - 40.535T + 0.11243T^2 - 1.0138 \times 10^{-4}T^3$ where T in K
$\lambda(T)$	$-0.58166 + 6.3555 \times 10^{-3}T - 7.9643 \times 10^{-6}T^2$ where T in K
ρ_s	2330
c_s	712
λ_s	148

4. Results and discussion

Fig. 3(a) depicts for constant heat flux $q^* = 0.4$ imposed, the variation of $\bar{T}_{\max}$ as a function of the coolant mass flow rate. For reliable operation of the electronics, in nondimensional value, the heat sink disc should be operating below SPT $\simeq 0.1488$, shown by horizontal line. It is obvious that to maintain the disc maximum temperature below SPT, compared to the straight channel case ($k = 0$), the critical minimum mass flow rate (M_{cr}) required by the tree shaped network is less. The degree of temperature reduction also reduces as one proceeds to higher level of complexity of the tree network (from $k = 1$ to 4).

The M_{cr} required for each level of complexity to operate the disc heat sink below SPT can be obtained from Fig. 3(a). Comparing the M_{cr} obtained for the configurations $n = 3$, $k = 1$ and $n = 3$, $k = 2$ with that of the one available in Wechsatol et al. [18], one can observe from Fig. 3(b), the similarity of the trend of thermal and flow resistance. However the configuration from Wechsatol et al. [18] predict a lesser thermal resistance ($\bar{T}$) than that of the present case, for identical flow rate (M). This is due to two reasons. The boundary conditions of the constant heat flux as imposed in the present case are different from that of the constant volumetric heat generation imposed in Wechsatol et al. [18]. The constant surface q^* imposed is a more appropriate boundary condition for modelling heat sinks attached to electronics using a substrate of finite material thickness. This requires the system to operate with a higher thermal resistance, caused by the heat diffusion across the heat sink from the surface where q^* is imposed to the cooling channel (see Fig. 1). The second reason that increases the thermal resistance is the $\mu(T)$ considered for the cooling fluid that reduces the convection heat transfer coefficient of the coolant flow.

For all levels of channel branching complexity with coolant flow kept at M_{cr}, Figs. 4(a) and (b) depict respectively the isotherms over the bottom surface of the disk and the circumferential average temperature along the radius of the disc from center to periphery. The dashed lines in Fig. 4(a) indicate the location of the branching of the trees for various levels of com-

Table 3
Grid independence study: $k = 2$, $n = 3$, $T_{\text{in}} = 300$ K, $\dot{m} = 3 \times 10^{-3}$ kg s^{-1}, $q'' = 100$ kW m^{-2}

S. no.	Total grid points	$T_{\max}$, K	Error $\Delta T_{\max}$ in percentage	Mass flux balance, kg s^{-1}	Error in energy $\frac{E_{\text{in}} - E_{\text{out}}}{E_{\text{in}}} \times 100$
1	164 038	349.4301	–	2.1275×10^{-13}	4.9100×10^{-6}
2	213 730	344.8983	1.2969	7.656×10^{-10}	6.5290×10^{-6}
3	311 158	344.8708	0.0078	8.1865×10^{-14}	5.4426×10^{-6}

Table 4
Time independence study for $k = 2$, $n = 3$, with grid size 311 158

S. no.	Time step Δt, s	Time taken to reach steady state, s	$T_{\max}$ (at the bottom surface of the chip) K	Error in percentage $\frac{\Delta T_{\max}}{\Delta t} \times 100$
1	0.5	25	344.8662	–
2	0.25	25	344.8638	−0.96
3	0.1	25	344.8747	10.9
4	0.05	25	344.8749	0.4
5	0.025	25	344.8750	0.4

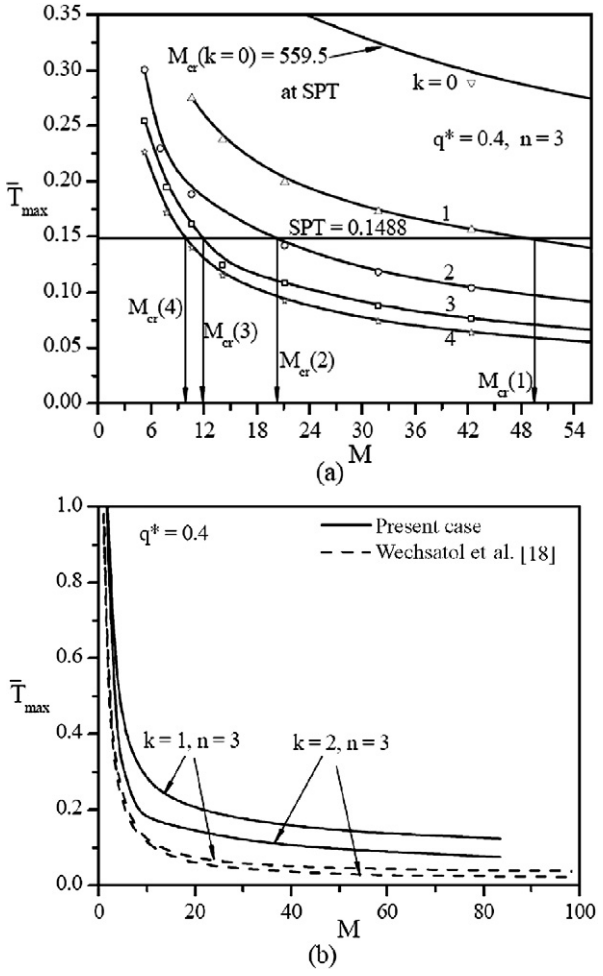

Fig. 3. (a) Steady state maximum temperature of the heat sink for several flow rates for all network levels considered for a constant imposed heat flux $q^* = 0.4$. (b) Comparison of present results with Wechsatol et al. [18] for the tree levels $k = 1$, $n = 3$ and $k = 2$, $n = 3$.

plexity (see Fig. 1). The increasing temperature towards the edge of the disk is expected in Fig. 4(a) (i to iv), irrespective of the complexity of branching, the dimensions of Table 1, as discussed in Wechsatol et al. [5], strives to keep the flow resistance minimum by the geometry of the branches. Hence the thermal resistance increases locally along the radial direction. On the other hand, although the disk heat sink is operating at a higher average temperature for higher levels of complexity (compare $k = 4$ with $k = 1$ in Fig. 4(b)), a more uniform temperature distribution is achieved ($\bar{T}_{\max} \to \bar{T}_{\text{avg}}$) as complexity of branching increases.

Upon testing the configuration for several values of imposed heat flux q^*, the corresponding M_{cr} that operates the disc below SPT during steady state is found for all levels of complexity ($k = 0$ to 4) and are given in Fig. 5. Except for lower values of q^*, the required M_{cr} varies almost linearly with q^* for all the levels ($k = 0$ to 4).

To highlight the importance of transient response under optimal flow (mass flow rate, M) and thermal resistance (maximum temperature of the sink $\bar{T}_{\max}$), the system behavior under non-optimal conditions is presented first. In Fig. 6, the time evolution of the $\bar{T}_{\max}$ at the bottom surface of the disk is plotted in nondimensional values for all levels of network complexity ($k = 0$ to 4) for an arbitrary coolant mass flow rate ($M = 42.39 \equiv \dot{m} = 3\ \text{g s}^{-1}$). It is apparent from Fig. 6 that the time taken to asymptotically reach steady state (calculated as the time for $\bar{T}_{\max}$ to reach 99.9 percentage of the steady state $\bar{T}_{\max}$) is different for different levels of complexities. However the constancy of the imposed mass flow rate M has rendered the systems with various k levels to operate with different thermal resistances. In other words, a non-optimal (arbitrary) flow resistance (M) offsets the optimality of the thermal resistance $\bar{T}_{\max}$ of the system, also in the transient situation. This can be rectified as shown in Fig. 7, where each of the system with different k levels of complexity, when imposed with identical heat load (fixed q^*), is supplied with the critical minimum mass flow rate, M_{cr}, setting the required respective optimal flow resistance.

Each of the set of curves grouped distinctly are for three different imposed heat flux values, while each group contains curves for each of the k values. What is more striking in Fig. 7 is the observation of the uniformity of the transient response of the system for all the levels of complexity k, when supplied with their respective M_{cr} values (similar $\bar{T}_{\max}$ values for each q^* with variation among them being less than 2 percentage), even though these M_{cr} values were obtained from their respective steady state results (Fig. 3).

Further, observing the other sets of curves one can conclude that this transient response of the system when operating under an optimal flow resistance (thereby optimal thermal resistance) is invariant to the imposed heat flux. The nondimensionalization of the $\bar{T}_{\max}$ on the ordinate renders the corresponding nondimensional SPT value lesser due to the presence of the q^* in the denominator (see nomenclature), but the dimensional SPT value is the same for all the cases tested. Hence, comparing with the sets of curves for $q^* = 0.2$, as expected, the time for reaching steady state (calculated as the time for $\bar{T}_{\max}$ to reach 99.9 percentage of the steady state $\bar{T}_{\max}$) for the set of curves imposed with $q^* = 0.4$ decreases.

At these critical mass flow rates, the transient evolution of the bottom surface average temperature $\bar{T}_{\text{avg}}$ is shown in Fig. 8, where as expected, the disk system with higher levels of branching complexity (thereby, more fluid flowing space) evolves into a lesser steady state temperature value.

The effect of providing a radial inclination for the microchannel network is next studied by providing inclinations of $(\bar{h}_{\text{out}} - \bar{h}_{\text{in}}) = \bar{h}_{\text{incl}} = 0.005$ and 0.0125. Figs. 9(a) and (b) show the effect of the radial inclination of the coolant channels on the pressure distribution along the path shown as a dotted line along the center of the channel in Fig. 2, for the channel levels $k = 1, 2$ and $k = 3, 4$ respectively. At each channel bifurcation point (see Fig. 2), the hydrodynamic boundary layer redevelops confining the pressure peaks to appear at these locations. The overall pressure drop however is less when compared to the configuration with zero radial inclination channel. As the number of levels (k) increases it results in more number of peaks formed along the radial direction of the flow, leading to lesser degree of pressure drop reduction because of the channel inclination. This effect is apparent in Fig. 10, where the channel inclination is shown

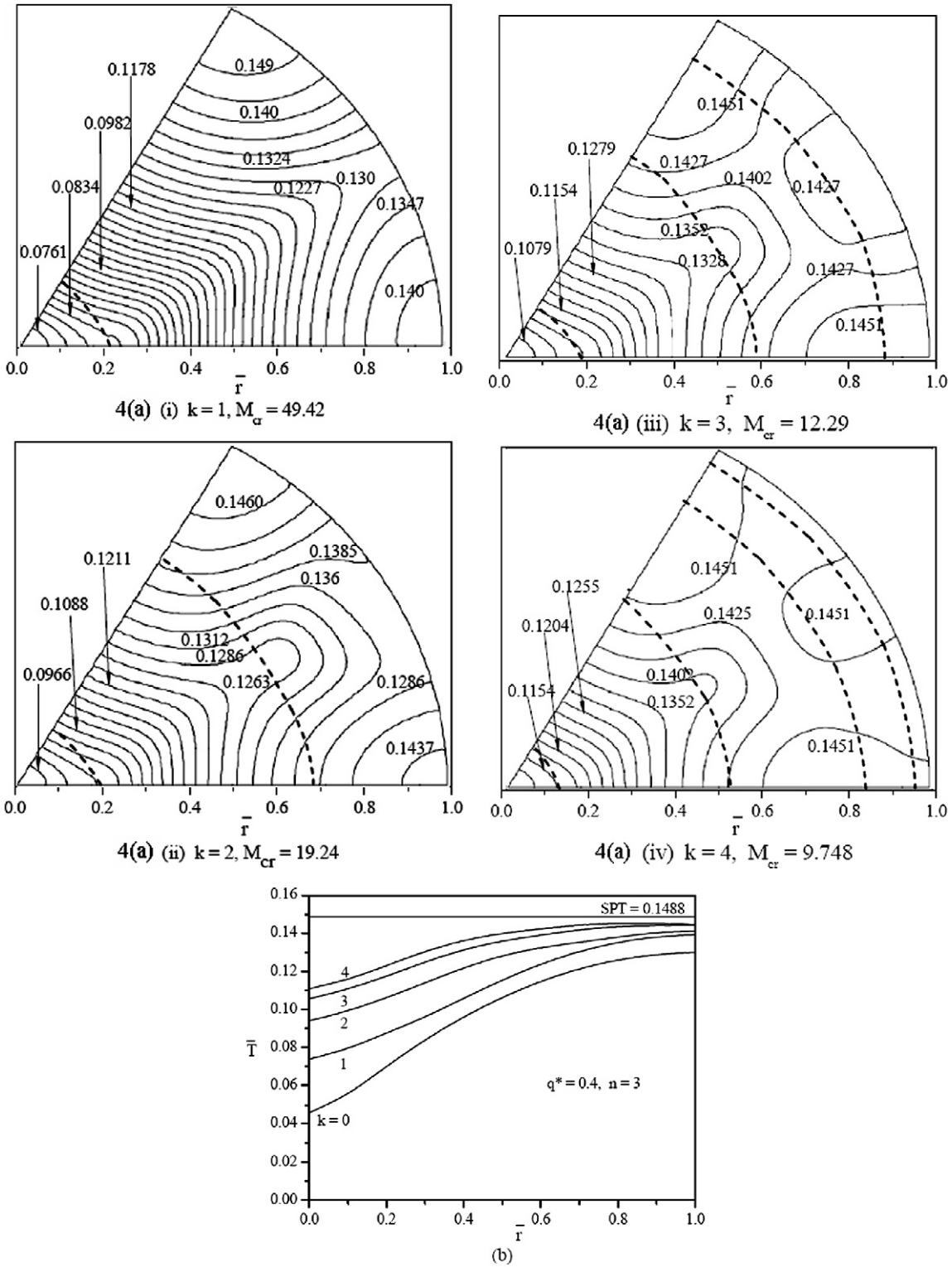

Fig. 4. (a) (i–iv) Steady state isotherms for all network levels at the bottom surface of the disk in Fig. 1. (b) The circumferential average (along the dashed line in Fig. 4(a)) temperature along the radius of the disk for identical parameters that resulted in Fig. 4(a).

with respect to heat flux for all levels of channel network complexity. Observing either a set of continuous ($\bar{h}_{\text{incl}} = 0.0125$) or dashed lines ($\bar{h}_{\text{incl}} = 0.005$) one can perceive the reduction in the pressure drop gained by channel inclination effect. Further as one could expect higher the inclination, higher the gain in the pressure drop observed, which however would be limited by manufacturing constraints of the heat sink.

Worth noting is the fact that the dependence of pressure drop gain because of inclination on the imposed heat flux is very weak even when thermophysical property variation for the

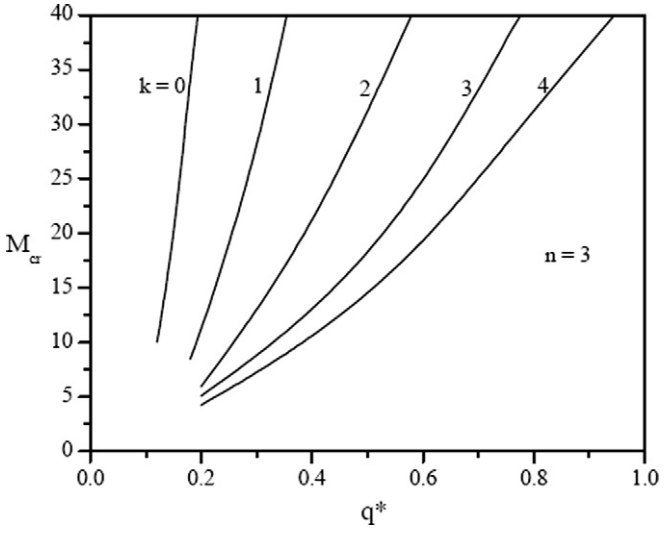

Fig. 5. The variation of heat flux with the mass flow rate for all levels.

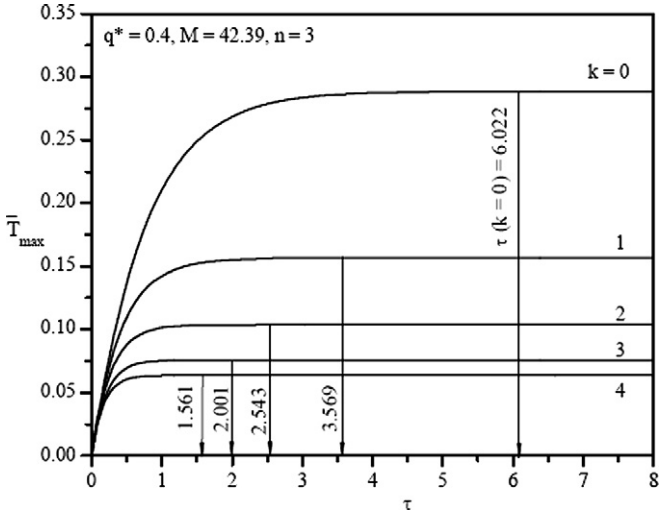

Fig. 6. Transient response of the $\bar{T}_{\max}$ (at the bottom of the disk) with $M = 42.39$ for all the tree levels.

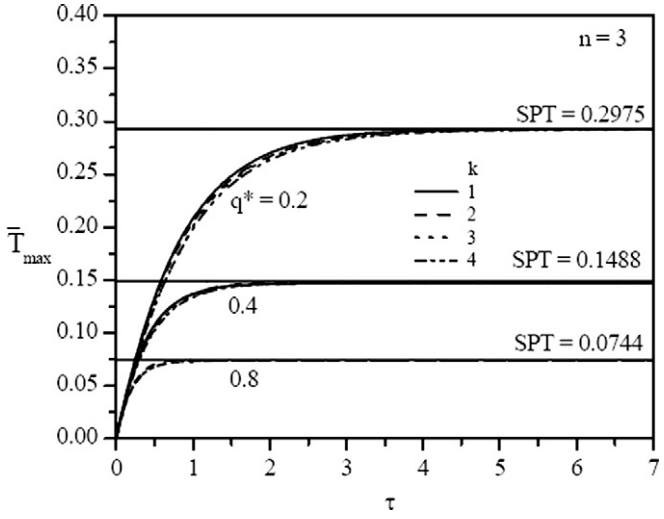

Fig. 7. The transient behaviour of maximum temperature of disk with critical mass flow rates of the tree levels 1 to 4.

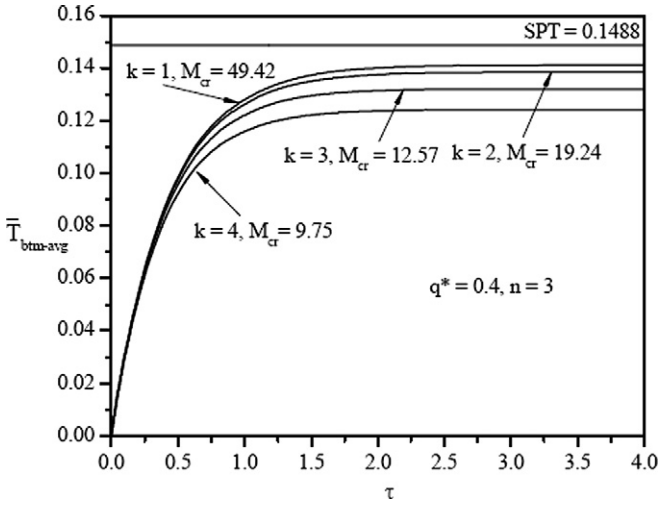

Fig. 8. The transient behaviour of average temperature of disk at bottom surface with critical mass flow rates of the tree levels 1 to 4.

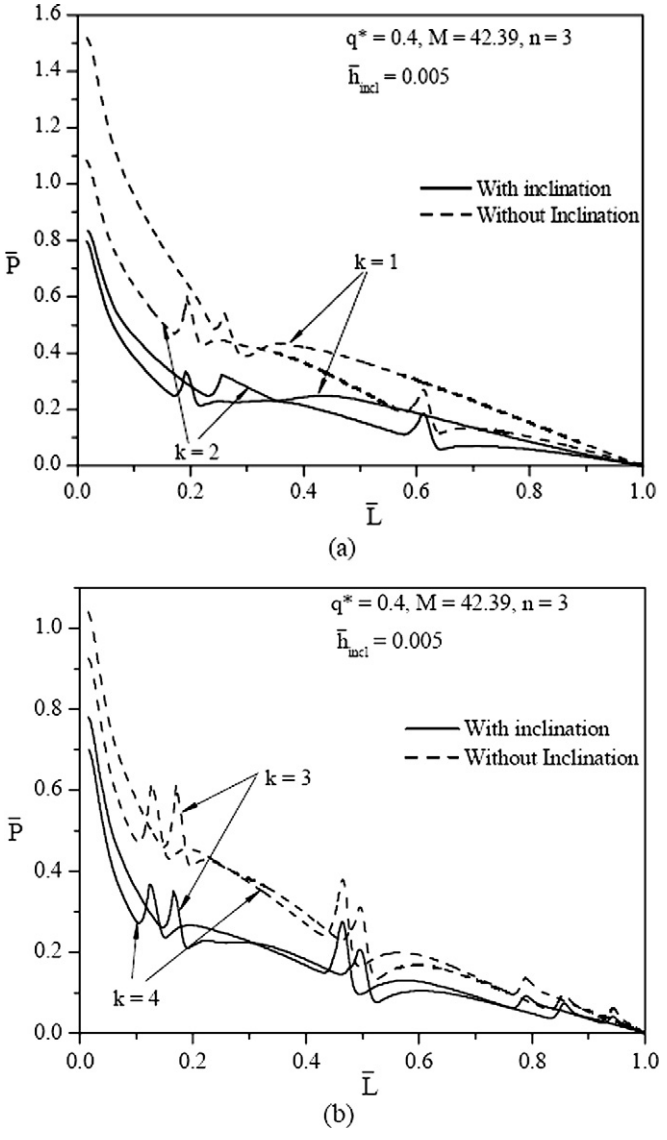

Fig. 9. The effect of channel inclination on the pressure distribution for all the tree levels (a) $k = 1$ and 2, $n = 3$ (b) $k = 3$ and 4, $n = 3$.

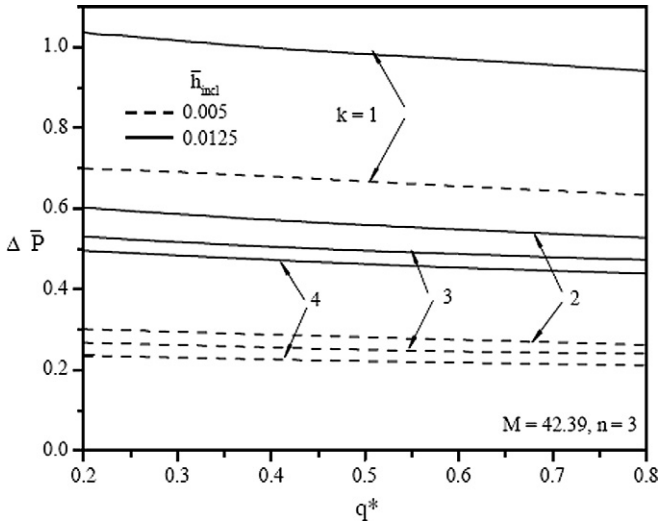

Fig. 10. The reduction in pressure between straight and inclined channel network with heat flux for all levels.

coolant flow ($\mu = \mu(T)$; $\rho = \rho(T)$; $\lambda = \lambda(T)$; $c_p = c_p(T)$; see Table 2) are taken into account. This suggests the use of channel inclination as design feature to have pressure drop incurred for higher levels of network complexity ($k = 3$ or 4) where one could anticipate more uniform temperature distribution (as shown in Figs. 3 and 4).

5. Conclusions

Tree-shaped branching micro-channel networks, embedded in a disk-shaped heat sink, are studied numerically. The conjugate heat transfer within heat sink is analyzed by considering heat conduction in the solid portion of the disc along with the forced convection of the cooling fluid.

Results show that increased complexity in the network geometry achieved with increased levels of branching of the fluid channels, decreases the maximum temperature ($\bar{T}_{\max}$) of the heat sink, when imposed with a constant heat flux. It further reduces the overall temperature difference ($\bar{T}_{\max} - \bar{T}_{\text{in}}$) resulting in a more uniform temperature distribution ($\bar{T}_{\max} \to \bar{T}_{\text{avg}}$) for the heat sink. To maintain the heat sink below the SPT and also to have uniform temperature one has to go for an increased branching level for a given typical mass flow rate.

Transient response of the disk with differing levels of tree complexities, using the steady state result for minimal flow resistance that yields minimal thermal resistance for heat transfer, was also investigated. Irrespective of the level of channel branching complexity, the transient thermal resistance of the cooling disk is shown to behave uniformly under similar imposed heat transfer load, allowing the heat sink disk to operate within the set point temperature (SPT = 90 °C) of the electronics being cooled. This is an useful engineering result as the electronics being cooling by these tree-network microchannel embedded disks would in practice be subjected to transient thermal condition during the periodic start-up or shut-down of the device.

Further, even though the disk operates at a more uniform spatial temperature ($\bar{T}_{\max} \to \bar{T}_{\text{avg}}$) for higher levels of complexity of the tree networks (for $k = 3$ or 4), the overall pressure drop also increases. It is shown here that an inclination of the microchannel tree network along the radial direction, irrespective of the level of complexity (k), reduces the overall pressure drop of the system. For instance, by allowing $\bar{h}_{\text{incl}} = 0.005$ inclination to the channel shows 45 percent reduction in pressure drop for the level $k = 1$, $n = 3$ and 25 percent for level $k = 4$, $n = 3$ as compared to the corresponding planar channel. With the reduced average temperature of the system for higher complexity of the geometry providing channel inclination is a viable option for increasing the performance of such networks.

References

[1] F. Incropera, Liquid Cooling of Electronic Devices by Single Phase Convection, John Wiley and Sons, New York, 1999.
[2] A. Bejan, Constructal-theory network of conducting paths for cooling a heat generating volume, Int. J. Heat Mass Transfer 40 (1997) 799–816.
[3] A. Bejan, Shape and Structure, from Engineering to Nature, Cambridge University Press, Cambridge, UK, 2000.
[4] A. Bejan, M.R. Errera, Convective trees of fluid channels for volumetric cooling, Int. J. Heat Mass Transfer 43 (2000) 3105–3118.
[5] W. Wechsatol, S. Lorente, A. Bejan, Optimal tree-shaped networks for fluid flow in a disc-shaped body, Int. J. Heat Mass Transfer 45 (2002) 4911–4924.
[6] W. Wechsatol, S. Lorente, A. Bejan, Tree-shaped networks with loops, Int. J. Heat Mass Transfer 48 (2005) 573–583.
[7] L.A.O. Rocha, S. Lorente, A. Bejan, Conduction tree networks with loops for cooling a heat generating volume, Int. J. Heat Mass Transfer 49 (2006) 2626–2635.
[8] D. Tuckerman, R. Pease, High-performance heat sinking for VLSI, IEEE Electron Dev. Lett. 2 (1981) 126–129.
[9] Y. Chen, P. Cheng, Heat transfer and pressure drop in fractal tree-like micro-channel nets, Int. J. Heat Mass Transfer 45 (2002) 2643–2648.
[10] S. Senn, D. Poulikakos, Laminar mixing, heat transfer and pressure drop in tree-like micro-channel nets and their application for thermal management in polymer electrolyte fuel cells, J. Power Sources 130 (2004) 178–191.
[11] X.Q. Wang, A.S. Mujumdar, C. Yap, Numerical analysis of blockage and optimization of heat transfer performance of fractal-like microchannel nets, J. Electronic Packaging 128 (2006) 38–45.
[12] C. Murray, The physiological principle of minimum work, in the vascular system, and the cost of blood-volume, Proc. Acad. Nat. Sci. 12 (1926) 20–214.
[13] D. Pence, K.E. Enfield, Inherent benefits in microscale fractal-like devices for enhanced transport phenomena, in: Collins, C.A. Brebbia (Eds.), Design and Nature, WIT Press, Rhodes, Greece, 2004, pp. 317–328.
[14] D. Liu, S. Garimella, Investigation of liquid flow in microchannels, AIAA J. Thermophys. Heat Transfer 18 (2004) 65–72.
[15] J. Judy, D. Maynes, B.W. Webb, Characterization of frictional pressure drop for liquid flows through microchannels, Int. J. Heat Mass Transfer 45 (2002) 3477–3489.
[16] W. Qu, I. Mudawar, Experimental and numerical study of pressure drop and heat transfer in a single-phase microchannel heat sink, Int. J. Heat Mass Transfer 45 (2002) 2549–2565.
[17] S. Patankar, Numerical Heat Transfer and Fluid Flow, Taylor and Francis, 1980.
[18] W. Wechsatol, S. Lorente, A. Bejan, Dendritic heat convection on a disc, Int. J. Heat Mass Transfer 46 (2003) 4381–4391.